JGR Oceans

RESEARCH ARTICLE
10.1029/2022JC018932

Thermal Responses in Global Marine Planktonic Food Webs Are Mediated by Temperature Effects on Metabolism

Kevin M. Archibald[1], Stephanie Dutkiewicz[2,3], Charlotte Laufkötter[4,5], and Holly V. Moeller[1]

[1]Department of Ecology, Evolution, and Marine Biology, University of California Santa Barbara, Santa Barbara, CA, USA, [2]Department of Earth, Atmospheric, and Planetary Sciences, Massachusetts Institute of Technology, Cambridge, MA, USA, [3]Center for Global Change Science, Massachusetts Institute of Technology, Cambridge, MA, USA, [4]Climate and Environmental Physics, University of Bern, Bern, Switzerland, [5]Oeschger Centre for Climate Change Research, University of Bern, Bern, Switzerland

Abstract Rising ocean temperatures affect marine microbial ecosystems directly, since metabolic rates (e.g., photosynthesis, respiration) are temperature-dependent, but temperature also has indirect effects mediated through changes to the physical environment. Empirical observations of the long-term trends in biomass and productivity measure the integrated response of these two kinds of effects, making the independent components difficult to disentangle. We used a combination of modeling approaches to isolate the direct effects of rising temperatures on microbial metabolism and explored the consequences for food web dynamics and global biogeochemistry. We evaluated the effects of temperature sensitivity in two cases: first, assuming that all metabolic processes have the same temperature sensitivity, or, alternatively, that heterotrophic processes have higher temperature sensitivity than autotrophic processes. Microbial ecosystems at higher temperatures are characterized by increased productivity but decreased biomass stocks as a result of transient, high export events that reduce nutrient availability in the surface ocean. Trophic dynamics also mediate community structure shifts resulting in increased heterotroph to autotroph ratios at higher temperatures. These ecosystem thermal responses are magnified when the temperature sensitivity of heterotrophs is higher than that of autotrophs. These results provide important context for understanding the combined food web response to direct and indirect temperature effects and inform the construction and interpretation of Earth systems models used in climate projections.

Plain Language Summary Warming oceans cause a myriad of changes to marine ecosystems, including both biological changes to the organisms themselves and physical changes to the environment. Here, we use mathematical models to isolate the effects of warming that arise directly from temperature's effect on metabolic rates, and the resulting changes to marine food webs and the global carbon cycle. We focus on how different metabolic rates (e.g., photosynthesis, grazing) may have different temperature sensitivities and the consequences of those differences on the overall thermal sensitivity of marine ecosystems. We found that marine food webs had higher productivity, but less overall biomass, when temperatures increase. These effects were amplified when grazing had greater temperature sensitivity than photosynthesis. Increased temperature also had effects on community and food web structure. These results provide important context for the kinds of global models that are used in climate change projections.

Key Points:

- Warming results in increased productivity, but decreased biomass, in marine microbial food webs due to the thermal dependence of metabolism
- Higher temperatures disproportionately favor higher trophic levels, increasing the ratio of heterotrophs to autotrophs
- Thermal responses are amplified if heterotrophic and autotrophic processes have different temperature sensitivity coefficients

Supporting Information:

Supporting Information may be found in the online version of this article.

Correspondence to:

K. M. Archibald,
karchibald@ucsb.edu

Citation:

Archibald, K. M., Dutkiewicz, S., Laufkötter, C., & Moeller, H. V. (2022). Thermal responses in global marine planktonic food webs are mediated by temperature effects on metabolism. *Journal of Geophysical Research: Oceans*, *127*, e2022JC018932. https://doi.org/10.1029/2022JC018932

Received 3 JUN 2022
Accepted 7 NOV 2022
Corrected 20 JAN 2023

This article was corrected on 20 JAN 2023. See the end of the full text for details.

1. Introduction

Over the past century, global average sea surface temperature (SST) has increased by 0.7°C (Bindoff et al., 2007). This surface warming has been accompanied by a steady increase in the heat content of the upper 2,000 m of the water column since at least the 1950s, with accelerating trends since 1991 (Cheng et al., 2019). Earth system model (ESM) projections predict additional increases in SST in the 21st century under all Representative Concentration Pathways (Bopp et al., 2013). In addition to increasing mean conditions, anthropogenic warming has caused unprecedented marine heatwaves in recent years, which are predicted to increase in both intensity and frequency (Frölicher et al., 2018; Laufkötter et al., 2020).

Rising ocean temperatures are expected to have significant impacts on pelagic plankton communities, which form the basis of marine food webs (Benedetti et al., 2021). The relatively short time scale of large spatial scale (e.g., satellite) observations makes it difficult to test this prediction because of challenges distinguishing between

climate-driven trends and natural ecosystem variability (Dutkiewicz et al., 2019; Henson et al., 2010). However, some empirical and modeling studies have indicated changes to phytoplankton biomass and primary productivity (Winder & Sommer, 2012). Global phytoplankton biomass has declined by about 1% of the global median value per year since the mid-twentieth century (Boyce et al., 2010), and global net primary productivity (NPP) has been declining since 1999, particularly in lower latitudes (Behrenfeld et al., 2006). Similarly, satellite observations have shown an increase in the extent of marine low-productivity zones since at least 1998, and the rate of expansion of these oligotrophic regions has been increasing in recent years (Irwin & Oliver, 2009; Polovina et al., 2008). Although observational data are still too short-term to definitively establish climate change-driven trends, modeling studies suggest that there are indeed ongoing significant changes occurring in chlorophyll *a*, productivity, and planktonic community structure (Benedetti et al., 2021; Bopp et al., 2005; Dutkiewicz et al., 2019, 2015; Kwiatkowski et al., 2020; Murphy et al., 2020).

Temperature-driven ecosystem changes arise from the cumulative effects of various mechanisms, including direct effects of temperature on the intrinsic biology of marine organisms and indirect effects from changes to the physical environment (Dutkiewicz et al., 2013; Taucher & Oschlies, 2011). Physical drivers of phytoplankton variability include temperature (Behrenfeld et al., 2006; Martinez et al., 2009), water column stratification and the associated reduction in nutrient availability (Behrenfeld et al., 2006; Falkowski et al., 1998; Martinez et al., 2009), and wind (Westerling et al., 2006). Here, we are interested in isolating the direct effects of temperature on planktonic food webs, independent of changes to the physical environment.

Temperature has a direct effect on marine organisms because metabolic processes are intrinsically temperature dependent. At the species level, organisms generally have a temperature optimum at which their growth rate is maximized, but the optimum temperature (and the maximum growth rate achieved at that temperature) varies between species (Edwards et al., 2016). When the thermal response curves of many species within a functional group are combined, the taxon-level maximum growth rates increase exponentially as a function of temperature. This monotonic relationship between temperature and maximum growth rate is evident in data that integrate growth rates across many species of phytoplankton (Eppley, 1972) or zooplankton (Rose & Caron, 2007). The temperature sensitivity of such groups of species (i.e., the rate of exponential growth of the temperature-metabolic rate curve) can be described using a Q_{10} temperature coefficient following Eppley (1972). The Q_{10} coefficient is defined as the amount a biological rate (e.g., growth rate) will increase with a temperature increase of 10°C (see Section 2.1).

Differences may exist in the temperature sensitivity of the growth rates of different planktonic taxa (Barton & Yvon-Durocher, 2019). For example, observational data indicate that heterotrophy may be more sensitive to temperature than phototrophy (López-Urrutia et al., 2006; Rose & Caron, 2007), though the thermodynamic mechanism is not fully understood (Rose & Caron, 2007). As a result, zooplankton growth rates exhibit greater temperature sensitivity than phytoplankton (Rose & Caron, 2007). Recent evidence also demonstrates that temperature sensitivity can vary between phytoplankton functional types, even within taxa with the same metabolic strategy (Anderson et al., 2021). In spite of this, most models that contribute to the Intergovernmental Panel on Climate Change (IPCC) projections have not accounted for differences in temperature sensitivity between taxa, despite evidence that such differences can have important effects on model conclusions (Laufkötter et al., 2015).

Here, we explore the mechanisms by which temperature directly affects marine microbial ecosystem provisioning (e.g., production, biomass, export) and community structure in the absence of indirect effects that accompany warming, including stratification, reduced nutrient supply, and changes to circulation. Within this framework, we also evaluate the effects of alternate assumptions concerning temperature sensitivity: first, that all metabolic rates have the same temperature sensitivity (same Q_{10} values), or that heterotrophic metabolic processes have increased temperature sensitivity (i.e., higher Q_{10} value) compared to autotrophic processes. We utilize a combination of modeling approaches including both global biogeochemical models and simplified heuristic box models simulated under highly idealized warming scenarios. This approach is designed to provide analytical tools to explore the ecological mechanisms that mediate the direct effects of temperature on plankton food webs. It is not intended to make predictions concerning ecosystem states under any future climate conditions.

We find that, as temperature increases, faster metabolic rates drive increased export via the biological pump. Steady-state ecosystems following a temperature increase were characterized by increased productivity, but reduced biomass, relative to present day temperature conditions. Warming also causes a shift in community structure that increased the ratio of heterotrophs to autotrophs in the plankton assemblage. Ecosystem-level

thermal responses are amplified, and more strongly favor higher trophic levels, when heterotrophy is assumed to have a larger temperature sensitivity than autotrophy.

2. Methods

This study examines the impact of increasing temperature on planktonic food webs. To isolate the direct effects of metabolism on temperature, we used Q_{10} scaling to approximate the relationship between photosynthesis/heterotrophy and temperature. We tested the impacts of this parameterization in two models: The Darwin Model (Follett et al., 2022), a global scale ecosystem model that allows us to quantify the impacts of thermal scaling across the world's surface oceans, and a simplified box model, which allows us to isolate specific mechanistic drivers of phenomena observed in the Darwin model.

2.1. Q_{10} Temperature Coefficients

To estimate the effects of temperature on metabolic rates, we used the same parameterization that is used in climate change simulation models, such as in the IPCC Coupled Model Intercomparison Project (CMIP6; Kwiatkowski et al., 2020). Similar to those models, we quantify the effects of temperature on ecosystem dynamics by parameterizing metabolic rates as exponentially increasing functions of temperature (following Eppley, 1972, Figure 1a). A metabolic rate, R, at a given temperature can be calculated from a known rate, R_0, at the reference temperature, T_0, and the Q_{10} temperature coefficient following,

$$R = R_0 Q_{10}^{(T-T_0)/10} \quad (1)$$

This equation assumes that metabolic rates increase monotonically as a function of temperature. Although this is not true of individual species, which have maximum thermal tolerances, here we model *communities* of organisms within a given functional group. Therefore, we have implicitly assumed that whenever a given species passes its thermal maximum, it will be replaced by a different species with a higher temperature range. This monotonic behavior can be seen in data sets that compile maximum growth rates as a function of temperature across many species (e.g., Bissinger et al., 2008; Eppley, 1972). There is evidence that phytoplankton communities near the equator are already nearing their thermal maximum and are therefore more vulnerable to increases in temperature (Thomas et al., 2012). However, we have chosen to simplify our representation of metabolic temperature sensitivity in favor of idealized cases. Importantly, this assumption of monotonicity is how the temperature sensitivity of metabolism is represented in the IPCC reports (CMIP6; Kwiatkowski et al., 2020; as well as earlier CMIP models), and so it is useful to do so here so that our results may inform that significant body of work. We investigated two cases of relative temperature sensitivity in autotrophs and heterotrophs (Table 1). First, we assumed that all metabolic processes (including photosynthesis, heterotrophy, and mortality) in the models have the same temperature sensitivity (1.88; Eppley, 1972). Second, and alternatively, we assumed that heterotrophs have a higher temperature sensitivity (2.7; Huntley & Lopez, 1992).

2.2. Darwin Model

To assess the effects of temperature on the upper ocean ecosystem, we performed simulations using the Darwin model (Figure 2). The Darwin simulations incorporate a coupled physical/biogeochemical/ecosystem model based on that used in Follett et al. (2022). Circulation and mixing are provided by the Massachusetts Institute of Technology (MIT) general circulation model (MITgcm; Marshall et al., 1997), constrained to be consistent with altimetric and hydrographic observations (Wunsch & Heimbach, 2007). This three-dimensional global configuration has coarse resolution (1° by 1° horizontally) and 23 depth bins ranging from 10 m in the surface to 500 m at depth. The biogeochemical/ecosystem component captures the cycling of C, N, P, Si, and Fe as they pass through inorganic and (dead and living) organic pools (Dutkiewicz et al., 2020, 2015). The specific details of the ecosystem follow from Follett et al. (2022) and resolve 31 phytoplankton (2 picoprokaryotes, 2 picoeukaryotes, 5 coccolithophores, 5 diazotrophs, 9 diatoms, 8 mixotrophic dinoflagellates), 16 zooplankton, and 3 heterotrophic bacteria. Phytoplankton have size resolution spanning from 0.6 to 140 μm ESD, zooplankton spanning 4.5 μm to 1,636 μm, and bacteria spanning 0.4–0.9 μm. Parameters influencing plankton growth, grazing, and sinking are related to size (Dutkiewicz et al., 2020), with specific differences between the six functional groups (Anderson

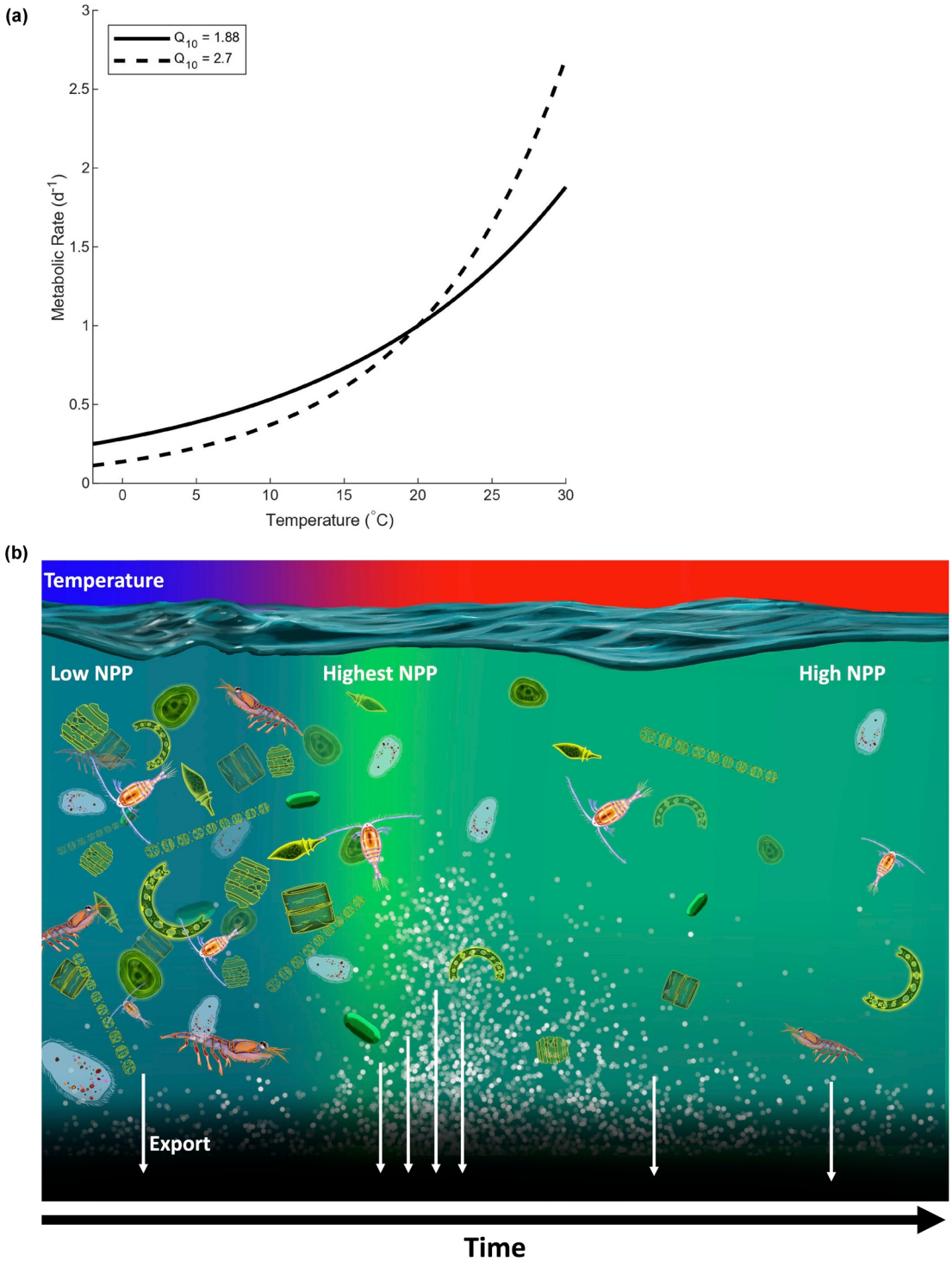

Figure 1. (a) Metabolic rates (e.g., photosynthesis, grazing) as a function of temperature using two different Q_{10} values. See Table 1 for the values used for autotrophic and heterotrophic metabolic processes in different model simulations. (b) A summary of the proposed mechanism: In the contemporary ocean (left side), phytoplankton (green) and zooplankton (orange) contribute to export (white arrows) to the deep ocean (black). A hypothetical, acute, and abrupt, increase in temperature causes an acceleration of all metabolic rates, leading to an increase in primary production (light green background) and an increase in biomass of phytoplankton and zooplankton. This increased biomass supports a transient increase in export, which drains nutrients from the surface ocean and causes the system to re-equilibrate at intermediate levels of primary production and lower levels of biomass. (Illustrated by Elise Cypher).

Table 1
Summary of Darwin Simulations

Experiment no.	ΔT(°C)	Temperature sensitivity case	Autotroph Q_{10}	Heterotroph Q_{10}
1	0	Same Q_{10}	1.88	1.88
2	1	Same Q_{10}	1.88	1.88
3	3	Same Q_{10}	1.88	1.88
4	5	Same Q_{10}	1.88	1.88
5	0	Different Q_{10}	1.88	2.7
6	1	Different Q_{10}	1.88	2.7
7	3	Different Q_{10}	1.88	2.7
8	5	Different Q_{10}	1.88	2.7

et al., 2021; Dutkiewicz et al., 2020). Phytoplankton growth is limited by multiple nutrients (N, P, Fe, and Si in the case of diatoms) and light (following Geider et al., 1998). For the purposes of calculating NPP, only the portion of mixotroph growth that comes from photosynthesis is included. Grazing by mixotrophs is considered "secondary production" and grouped with grazing by other heterotrophic consumers.

Grazing is parameterized using a Holling Type II functional response (Holling, 1965) and is size-specific such that grazers can prey upon plankton 5–15 times smaller than themselves, with an optimal size of 10 times smaller (Hansen et al., 1997; Kiørboe, 2018; Schartau et al., 2010). The emergent size distribution of the simulated plankton populations is strongly controlled both by the rate of supply of limiting nutrients (bottom up) and by grazing (top down; Dutkiewicz et al., 2020; Follett et al., 2022). The output from the simulation of Follett et al. (2022) compared well to annual and seasonal observations of chlorophyll-*a*, nutrients, and size and biogeochemical functional group distributions of phytoplankton (Buitenhuis et al., 2013; Ward, 2015). See further discussion in the appendix of Follett et al. (2022).

Mortality comes from grazing and an inherent quadratic mortality term that is small for all plankton size classes except the largest size class, where it serves as a closure term. Organic matter is remineralized by heterotrophic bacteria and an additional remineralization term that is not dependent on any biological component. Export occurs via sinking particles, whose sinking speed is size dependent, and by physical transport mediated by circulation. All biological rates (nutrient uptake, grazing, mortality, and remineralization) in Darwin have temperature dependence and follow the thermal scaling law described in Equation 1. The only difference between the simulation of Follett et al. (2022) and here is in the exact treatment of thermal responses of the biological rates. In Follett et al. (2022), phytoplankton growth Q_{10} was based on different functional groups as found in compilation of laboratory experiments in Anderson et al. (2021). Here, instead, we set all phytoplankton growth response to a

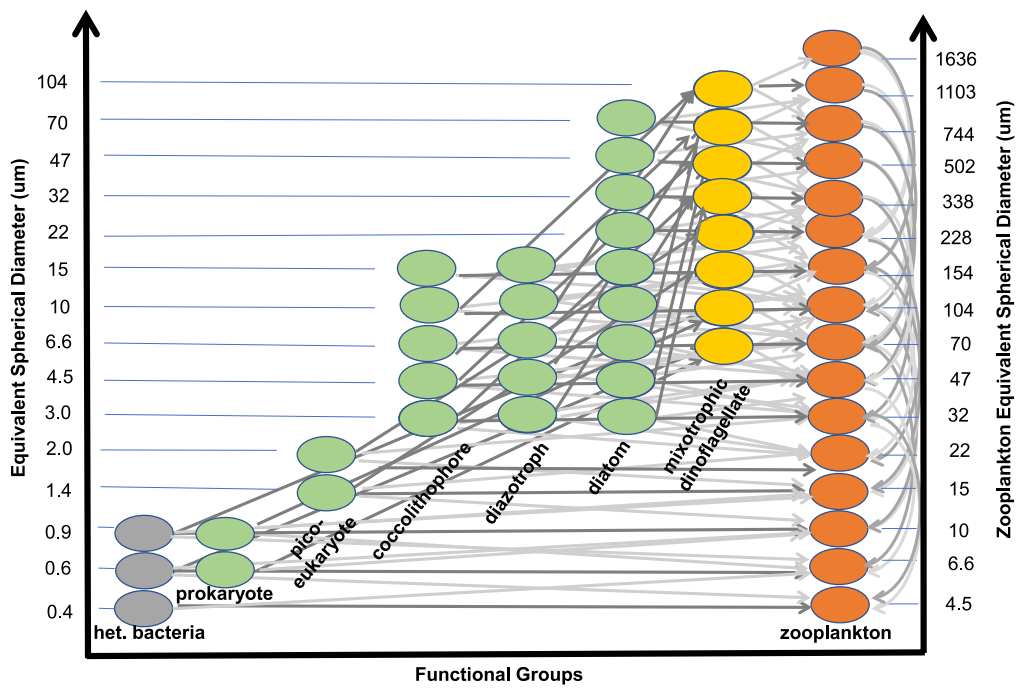

Figure 2. Size classes and functional groups in the Darwin model. The equivalent spherical diameter of each of the 50 resolved plankton types is shown, including bacteria (gray), phytoplankton (green), mixotrophic dinoflagellates (yellow), and zooplankton (orange). Zooplankton are plotted on a separate size axis. The grazing relationships between the different size classes is indicated by arrows, with darker arrows corresponding to higher grazing preference.

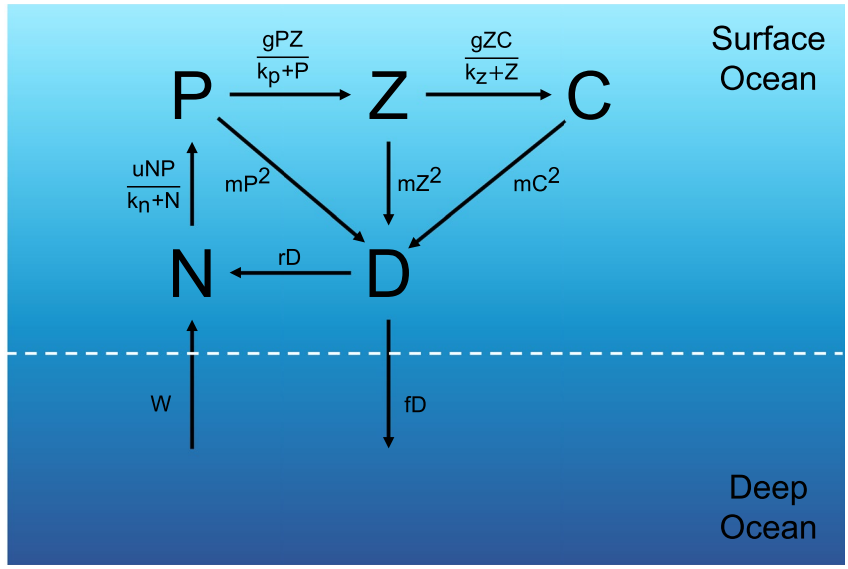

Figure 3. Food Web Box Model. The box model represents the relationships between a nutrient (N), a phytoplankton population (P), a zooplankton population (Z), a carnivore population (C), and a pool of organic matter (D) in the surface ocean. Arrows represent mass fluxes between model compartments. Mass is removed from the model by an export flux proportional to the detritus concentration (fD) and nutrients are supplied back to the surface ocean by upwelling (W).

Q_{10} of 1.88 (following Eppley, 1972), and a Q_{10} of grazing to either 1.88 or 2.7 following Table 1. Mortality and remineralization rates are also assigned a Q_{10} of 1.88 for both temperature sensitivity scenarios.

To quantify the effects of temperature on ecosystem structure, we ran a series of experiments of 10 yr duration, beginning with the same initial conditions (World Ocean Atlas for nutrients, and previous model output for all organic matter). The ecosystem quickly (within approximately 3 yr) reaches a quasi-steady state, meaning that the system maintains a repeated seasonal cycle from year to year. Here, we show results from the 10th yr of the simulations. In the series of experiments, the physical circulation and mixing remained identical, but the temperatures that the biological rates experience were altered: in each simulation the temperature was raised at each location, depth, and each time by a specific amount ($\Delta T = 1°C, 3°C, 5°C$, see Table 1). These experiments are thus highly idealized and designed specifically to interrogate the direct impact of increasing temperature on biological rates alone. The representation of warming has been abstracted and includes large increases in temperature on the upper end of predictions for warming over the next century (Kwiatkowski et al., 2020). Though there are slight differences in the community composition relative to Follett et al. (2022) given the differences in Q_{10} for plankton growth, the default simulation (i.e., where $\Delta T = 0°C$) compares similarly well to observations of chlorophyll-*a*, nutrients, and size distribution of phytoplankton and functional groups.

2.3. Box Model

To provide mechanistic context to the more complex, dynamical Darwin model, we also employed a simplified box model of the marine food web in the upper ocean (Figure 3). In this model, the surface ocean is represented as a well-mixed box that contains a single nutrient resource (N), a population of phytoplankton (P), a population of zooplankton (Z) that graze on the phytoplankton, a population of carnivores (C) that graze on the zooplankton, and a pool of detrital organic matter (D). The rate of change of nutrients in the surface ocean depends on the balance between upwelling from the deep ocean, remineralization of detritus, and uptake by phytoplankton. Nutrients are supplied to surface ocean via a fixed upwelling flux, W, and by remineralization of the organic matter with rate r. Nutrients are removed by phytoplankton uptake, which follows Monod dynamics with maximum uptake rate u and half-saturation coefficient k_n,

$$\frac{dN}{dt} = W + rD - \frac{uNP}{k_n + N}. \quad (2)$$

Table 2
Model Symbols and Their Meanings

Symbol	Description	Typical units	Simulation values
Variables:			
N	Inorganic nutrients	mmol C m^{-3}	
P	Phytoplankton	mmol C m^{-3}	
Z	Zooplankton	mmol C m^{-3}	
C	Carnivore	mmol C m^{-3}	
D	Detritus	mmol C m^{-3}	
Parameters:			
u	Nutrient uptake rate	d^{-1}	1.0
g	Grazing rate	d^{-1}	1.0
k_n	Nutrient uptake half-saturation	mmol C m^{-3}	0.2
k_p	Grazing half-saturation	mmol C m^{-3}	5
k_z	Carnivory half-saturation	mmol C m^{-3}	5
m	Mortality rate	d^{-1}	0.1
r	Remineralization rate	d^{-1}	0.7
f	Export ratio		0.1
W	Upwelling flux	mmol C m^{-3} d^{-1}	0.1

Phytoplankton growth is determined by the balance between nutrient uptake and mortality terms. Phytoplankton mortality includes both grazing by zooplankton, which follows Monod dynamics using a maximum grazing rate g and half-saturation coefficient k_p, as well as a quadratic mortality term (m) to represent density-dependent loss from outside sources,

$$\frac{dP}{dt} = \frac{uNP}{k_n + N} - \frac{gPZ}{k_p + P} - mP^2. \quad (3)$$

Zooplankton growth rate is determined by grazing on phytoplankton minus grazing by the carnivore and density-dependent mortality,

$$\frac{dZ}{dt} = \frac{gPZ}{k_p + P} - \frac{gZC}{k_z + Z} - mZ^2. \quad (4)$$

Carnivore growth rate is determined by grazing on zooplankton minus density-dependent mortality,

$$\frac{dC}{dt} = \frac{gZC}{k_z + Z} - mC^2. \quad (5)$$

Organic matter is added to the detrital pool through mortality terms, and removed via remineralization and export. The export rate, f, represents the sinking of biogenic particles out of the surface ocean,

$$\frac{dD}{dt} = mP^2 + mZ^2 + mC^2 - rD - fD. \quad (6)$$

For the purpose of calculating ecosystem provisioning fluxes in the box model, NPP is defined as $uNP/(k_n + N)$ and export is defined as fD. The model parameters were chosen to be similar to the more complex Darwin model (Table 2). Temperature dependence was added to the following biological rates: u, g, m, and r, following Equation 1. We simulated the model under the same two assumptions on Q_{10} between trophic levels: first, we assumed that all rate parameters had the same temperature sensitivity ($Q_{10} = 1.88$), and second, we assumed that the heterotrophic rates had a higher temperature sensitivity ($Q_{10} = 2.7$). Similar to the Darwin model, the results of this box model were examined under temperature increases ranging from +0°C to +5°C and were used to consider transient behavior following a temperature increase. We also leveraged the box model to conduct sensitivity tests on our results to the thermal dependence of other rates (mortality, remineralization).

3. Results

3.1. Higher Temperatures Lead to Declines in Biomass Despite Increased Productivity

First, we quantified the effects of thermal change on ecosystem provisioning in the Darwin model (Figure 4). Increasing temperatures resulted in higher NPP across the globe in both temperature sensitivity cases. However, despite the increase in productivity, total ecosystem biomass summed across all plankton types decreased. The largest changes in biomass occurred in high latitudes where phytoplankton and zooplankton abundance is typically high. The biomass decline was substantially larger in the case where the heterotrophic Q_{10} is larger than the autotrophic Q_{10}. Both the increase in NPP and the decrease in biomass were proportional to the temperature change (Figures 5a and 5b). The direction of these trends was the same for both Q_{10} cases, but the magnitude of the response was larger when we assumed that the Q_{10} for heterotrophic metabolic processes was larger than the Q_{10} for autotrophic processes.

More productive ecosystems may contain lower biomass for two reasons: (a) biomass accumulated in the non-living components of the model (e.g., inorganic nutrients, detritus) or (b) biomass was removed from the surface ocean along export pathways, such as the biological pump. To distinguish between compensatory mass redistribution and increased export, we used phosphorus as a mass-conserved tracer, tracking changes in the phosphorus content of inorganic nutrients, living biomass, and the detrital pool as temperature increased. Other

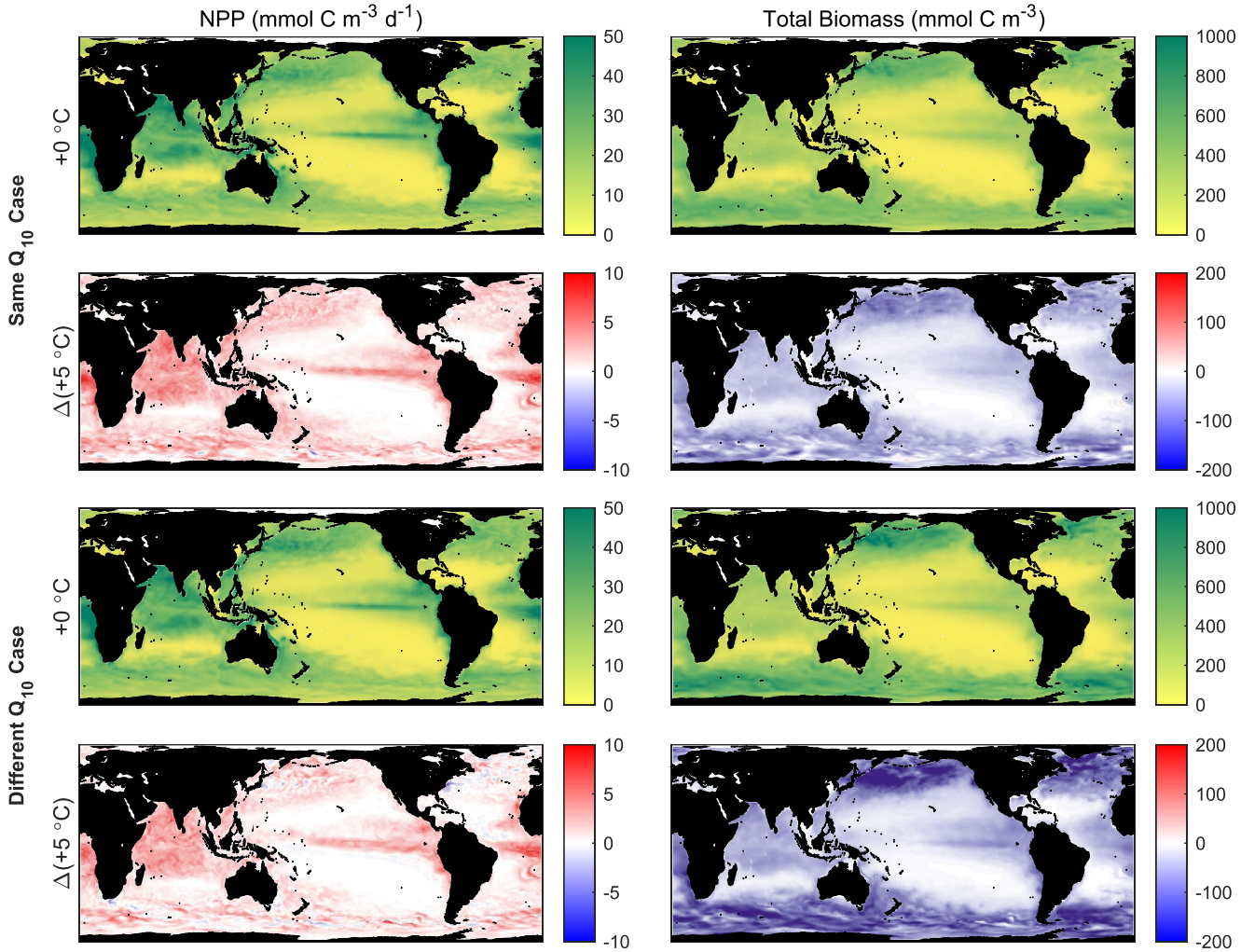

Figure 4. Annual mean depth-integrated net primary productivity (NPP; left column; mmol C m^{-2} d^{-1}) and total ecosystem biomass (right column; mmol C m^{-2}) in the Darwin model from the tenth year of the simulation for both temperature sensitivity cases (top, same Q_{10} values; bottom, different Q_{10} values). The net change between the +0°C and +5°C experiments are plotted to quantify the thermal response of each variable. In both cases, NPP increases globally while total ecosystem biomass decreases. The decline in biomass is amplified in the case where the heterotrophic Q_{10} is larger than the autotrophic Q_{10}.

elements, notably N and Fe, are less useful as a diagnostic due to additional source and loss terms (e.g., aeolian deposition, nitrogen fixation). While there were differences between the two temperature sensitivity scenarios, in both cases the total P content of the upper ocean declined significantly (Figure 6). This decline provides evidence of an increase in export (sustained or transient) at some point along the trajectory of the simulation.

3.2. Transient Increases in Export Drive Biomass Reductions

Synthesizing the evidence from the suite of Darwin simulations, we propose the following mechanism for direct temperature effects on marine planktonic food webs (Figure 1b). Warming drives higher productivity via accelerating metabolic rates. Increased productivity results in faster rates of export out of the surface ocean via the biological pump. Increased export, in turn, reduces the total nutrient availability in the surface ocean, resulting in a reduction in total biomass. The Darwin simulations were conducted for 10 yr, so the timescale of interest for this proposed mechanism is both ecologically relevant and small compared to large-scale circulation processes.

To explore this mechanism in greater detail, and evaluate the relative impacts of the thermal dependence of different processes relative to productivity (grazing, mortality, remineralization), we turn to the simplified box model. Transient behavior plays a key role in establishing the overall ecosystem thermal response (Figure 7).

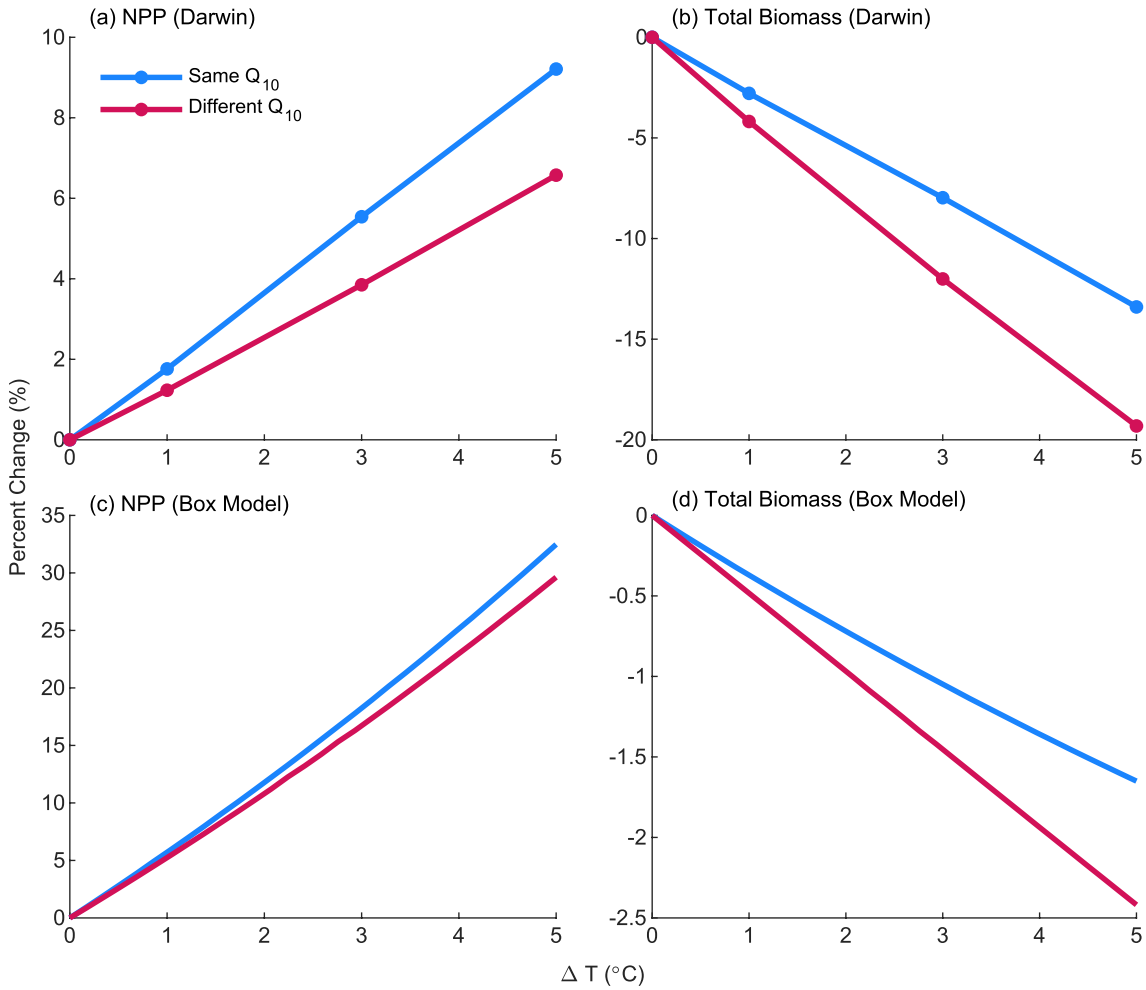

Figure 5. Thermal response curves for depth-integrated net primary productivity (NPP) (a and c) and total ecosystem biomass (b and d) in Darwin (a and b) and the box model (c and d) plotted as the percent change in each variable relative to the +0°C experiment. The data from the Darwin simulations represent globally integrated values. Each temperature sensitivity case is plotted as a separate line. In both models, NPP increases with temperature while biomass decreases. These trends are amplified in the case where the heterotrophic Q_{10} is larger than the autotrophic Q_{10}. Note that the *y*-axis scale is different between the two models and reflects a difference in the magnitude of the thermal response.

Immediately after the increase in temperature, all biological rates increase following metabolic scaling laws. This includes productivity across all trophic levels, plankton mortality, and remineralization. Increased productivity and mortality direct more biomass into the detrital pool. Increased detritus is partially accounted for by higher remineralization rates, however, it also results in an increased export flux, even though the export ratio is not directly affected by temperature. The modest increase in the export flux accounts for the observed reduction in total nutrient availability and, ultimately, the reduction in biomass. The direction of the trends in NPP and total biomass are the same in both the Darwin and box models (Figure 5), with NPP increasing and biomass decreasing as a function of temperature under both sensitivity cases. Also replicated by the box model is the characteristic that assuming different Q_{10} values for heterotrophic and autotrophic processes amplifies the ecosystem thermal response.

Steady-state dynamics in the box model represent a delicate balance between multiple, temperature-sensitive processes (productivity and grazing on one side and mortality and remineralization on the other) and the thermal responses in the box model provide insight into the relationship between these different rates. The biomass changes in the case in which all the Q_{10} values are the same are relatively small and represent a close-coupling of all the biological processes. Here, we have explored the relative effects of photosynthesis and grazing with our alternative Q_{10} scenarios, but mortality and remineralization are also temperature dependent and have the potential to vary in sensitivity relative to productivity. Generally speaking, the positive thermal dependence of

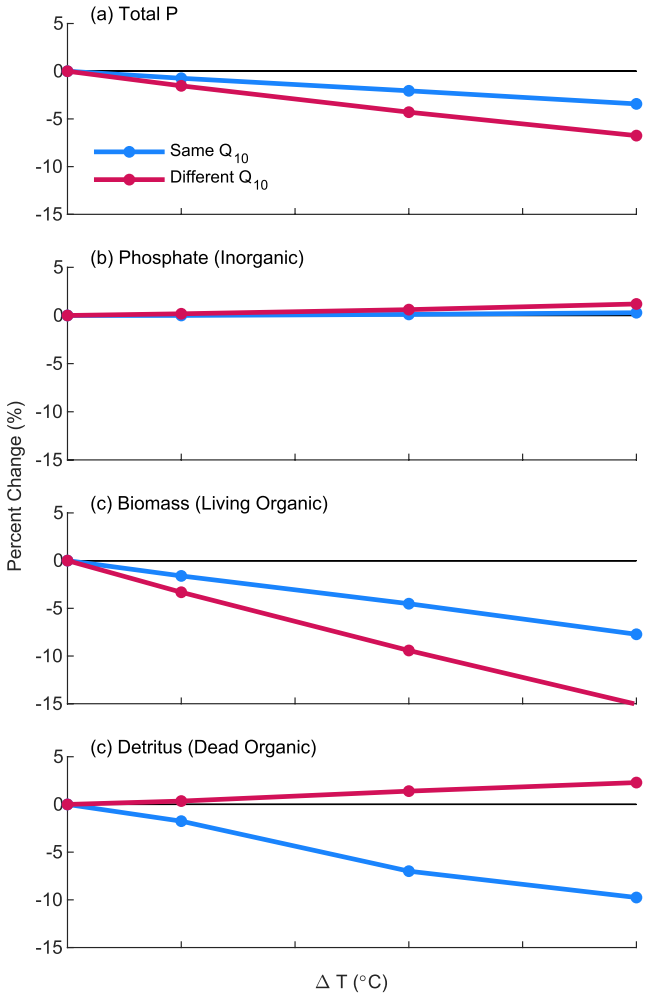

Figure 6. Proportional change in total P content at the surface (0 m) within different ecosystem components as a function of temperature in both temperature sensitivity cases: (a) total ecosystem P, (b) inorganic phosphate, (c) living organic P, and (c) dead organic P. The decline in total ecosystem P in the surface ocean indicates an increase in export.

these terms helps to buffer the biomass changes driven by temperature by balancing the accumulation of biomass in the detrital pool (Figures S1–S3 in Supporting Information S1).

3.3. Thermal Responses Include Community Structure Changes

The changes to bulk ecosystem provisioning characteristics (i.e., NPP and biomass) were accompanied by shifts in the community structure that resulted in more heterotrophic biomass relative to autotrophic biomass. Simulations of the box model suggest that this shift occurs in both temperature sensitivity cases, despite differences in the trophic level-specific biomass trends (Figure 8). In the case where the Q_{10} values are all the same, all trophic levels decrease at higher temperatures. However, phytoplankton decrease more than zooplankton and carnivores, leading to an increase in the ratio of heterotrophs to autotrophs (Figures 8a and 8c). In the case where the heterotrophic Q_{10} value is higher, the carnivore actually increases with temperature, resulting in a similar increase of heterotrophs relative to autotrophs (Figures 8b and 8d).

These results are mirrored in the Darwin simulations, using plankton functional type as a proxy for trophic level (Figure 9). In the "same Q_{10}" case, we observed declines in biomass across all functional types with larger declines farther down the food chain. When the heterotrophic Q_{10} was higher, however, the large zooplankton (which tend to be more carnivorous) increased at higher temperatures, while all other functional types declined. The net result of all the individual functional type changes is an increase in the ratio of heterotrophs to autotrophs. Within the autotrophic plankton functional types, there were community structure changes as well. Picoplankton declined much less than the larger-bodied diatoms in all experiments (Figure 9) and even increased in abundance in some locations (Figure S4 in Supporting Information S1), despite the overall negative trend.

The Darwin model showed significant regional differences in the community changes across different biogeochemical regimes (Figure 10). For example, in the high-latitude Southern Ocean, a 5°C increase was sufficient to allow some larger-bodied size classes to persist where they were previously unable to due to prohibitively low temperatures. The appearance of these larger size classes can cause local increases for certain functional types, even when the global trend is negative. Mixotrophic dinoflagellates showed especially high spatial variability compared to both pure autotrophs and pure heterotrophs. This is likely due to their complex metabolism and intermediate size that encourages many inter-type interactions, maximizing the potential for ecological feedbacks.

The relative changes in different functional types across multiple trophic levels also creates the potential for trophic cascades. Evidence for this can be seen by comparing the size-class specific thermal responses in locations with food chains of different lengths (Figure 11). At the scale of individual size classes, biomass changes tend to alternate between positive and negative moving down the food chain, with the largest size classes at the top of the food chain typically seeing increases. Specific size classes that increase in one location may decrease in another location because the food chain is a different length (Figure 11). This is consistent with the overall trend that higher temperatures benefit the highest trophic level, but which size class is at the top of the food chain may vary from place to place. Of course, size class is not a perfect proxy for trophic level in the Darwin model, given the complexity of grazing relationships (Figure 2). Furthermore, the specific differences between different functional types within the same trophic level introduces additional complexity to these patterns (Figure S5 in Supporting Information S1).

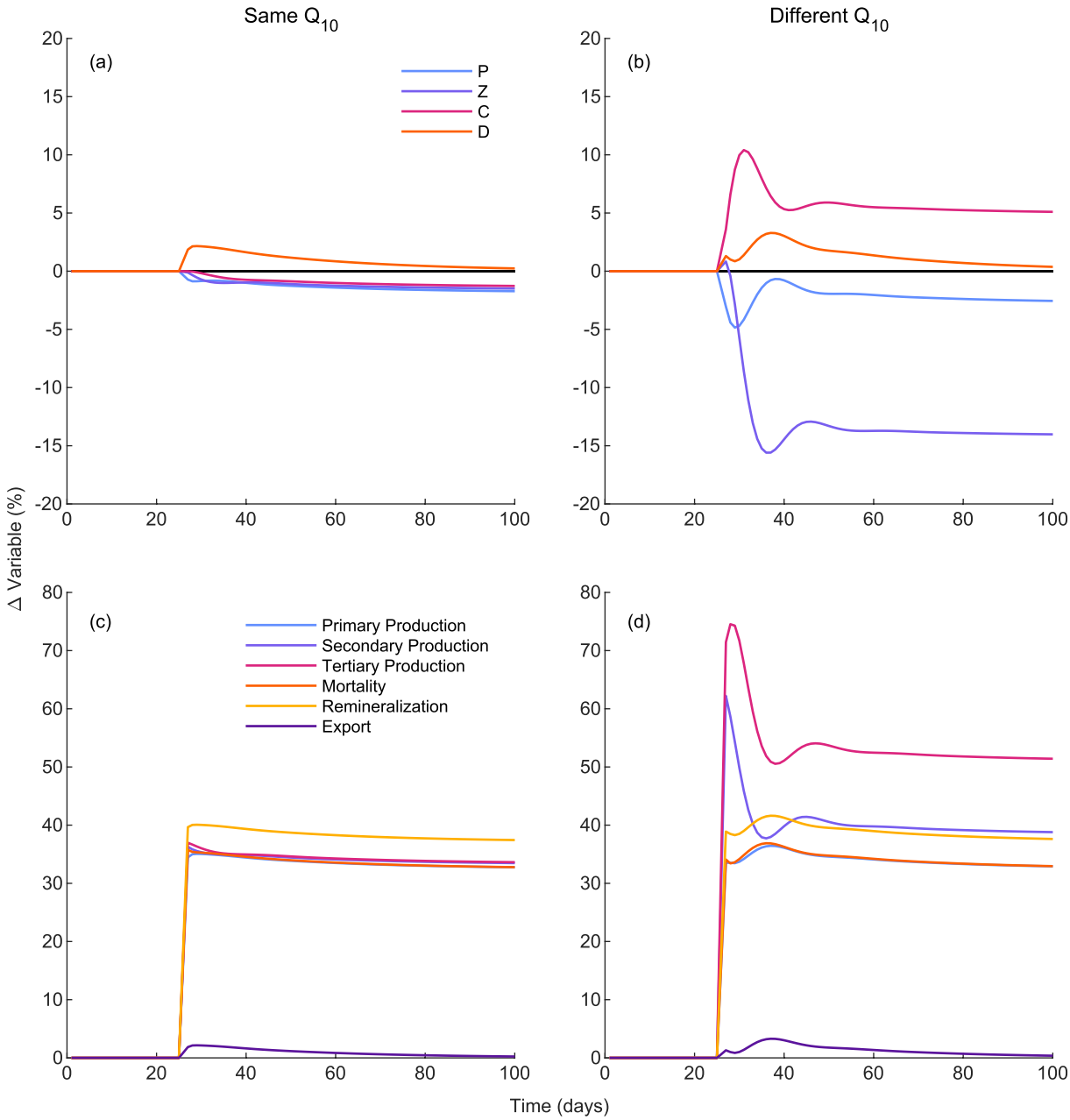

Figure 7. Time series of the box model showing transient behavior in model variables (a, b) and fluxes (c, d) for both temperature sensitivity scenarios as the model converges to a new equilibrium following an instantaneous temperature increase of 5°C at $t = 25$.

4. Discussion

The oceans' ecosystems are responding to multiple changes that accompany anthropogenic climate change, including warming, reduced sea-ice, alterations to the supply of nutrients, changes to the light environment, and ocean acidification. Here, we specifically target ecosystem-level changes caused by the direct effect of warming on metabolic rates. Rising ocean temperatures are expected to accelerate the metabolic rates of marine organisms. However, we show that even this relatively simple positive relationship between temperature and metabolic rate does not translate to easily predictable thermal responses at the ecosystem level. Increased productivity driven by warming results in additional export of material out of the surface ocean, resulting in ecosystems that are more productive, but contain less biomass, as the temperature increases. These results are consistent with observations of the thermal response of plankton communities in mesocosm experiments, which have empirically shown that

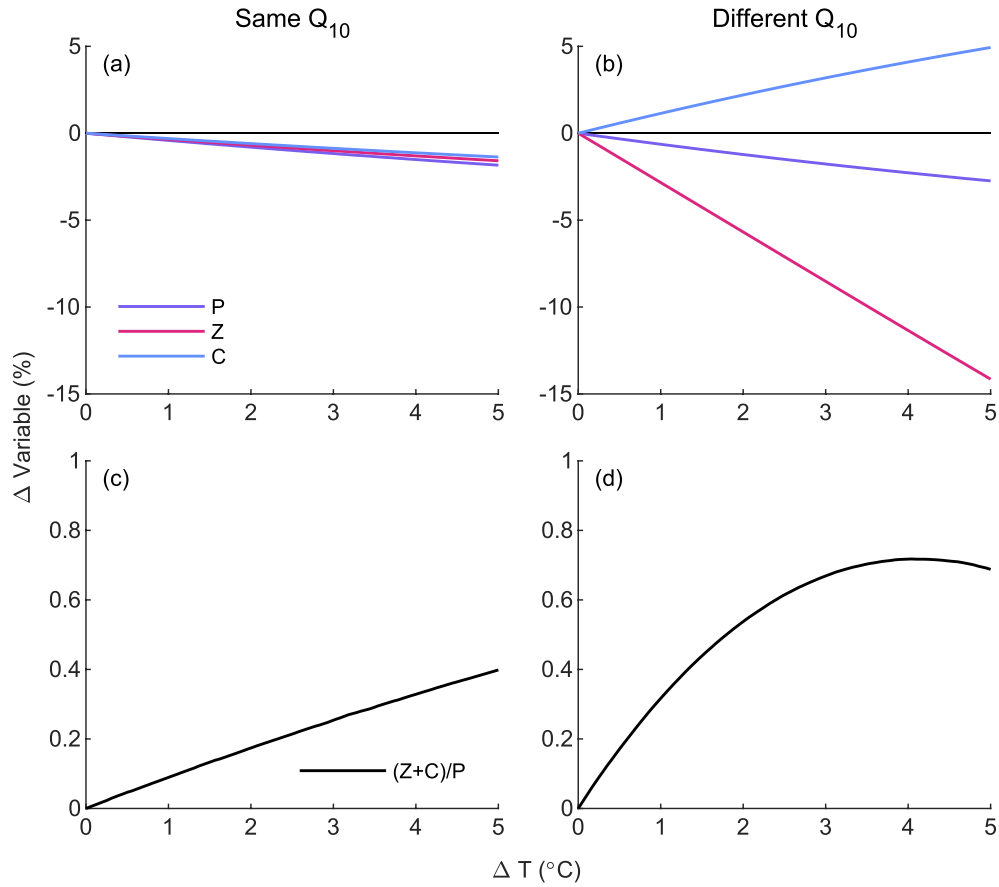

Figure 8. Proportional changes in the community structure of the box model as a function of temperature for both temperature sensitivity cases ((a and c), all Q_{10} values equal; (b and d) heterotrophic Q_{10} higher). In the case in which the autotrophic and heterotrophic Q_{10} values are the same, all trophic levels decline with temperature. However, when the heterotrophic Q_{10} is larger than the autotrophic Q_{10}, the top trophic level increases at higher temperatures, while the lower trophic levels decline significantly more. In both cases, however, the ratio of heterotrophs to autotrophs is positively related to temperature.

warming can drive declines in phytoplankton biomass despite the positive effect of temperature on productivity (Klauschies et al., 2012; Lewandowska & Sommer, 2010; O'Connor et al., 2009).

Warming also broadly drives community structure changes that result in increased abundances of heterotrophs compared to autotrophs. Both modeling and empirical studies have shown that the consumer-resource interaction can strengthen as an effect of increasing temperature (Gilbert et al., 2014; O'Connor, 2009). Such strengthening will benefit the trophic level at the top of the food chain most strongly. In our case, the highest trophic level was carnivorous zooplanktivores; the real ocean, however, contains additional higher-level consumers. Whether or not the temperature-driven gains are passed all the way up the food chain is unclear, and likely depends on the relative temperature sensitivities at each trophic level.

Although autotrophs as a whole declined in our simulations, we did observe a relative increase in small-bodied picoplankton relative to large-bodied diatoms. The shift toward smaller phytoplankton types is a classic thermal response in oceanography that has been proposed as a universal biological response to warming (Gardner et al., 2011; Yvon-Durocher et al., 2011). Water column stratification and reduced nutrient supply are often suggested as proximate causes of this decline in mean body size (Lewandowska et al., 2014; Morán et al., 2010; O'Connor et al., 2009). Here, we have found a similar result using the direct effects of temperature alone, suggesting this trend may occur due to changes in grazing pressure or nutrient availability that occur as a result of shifts in community structure.

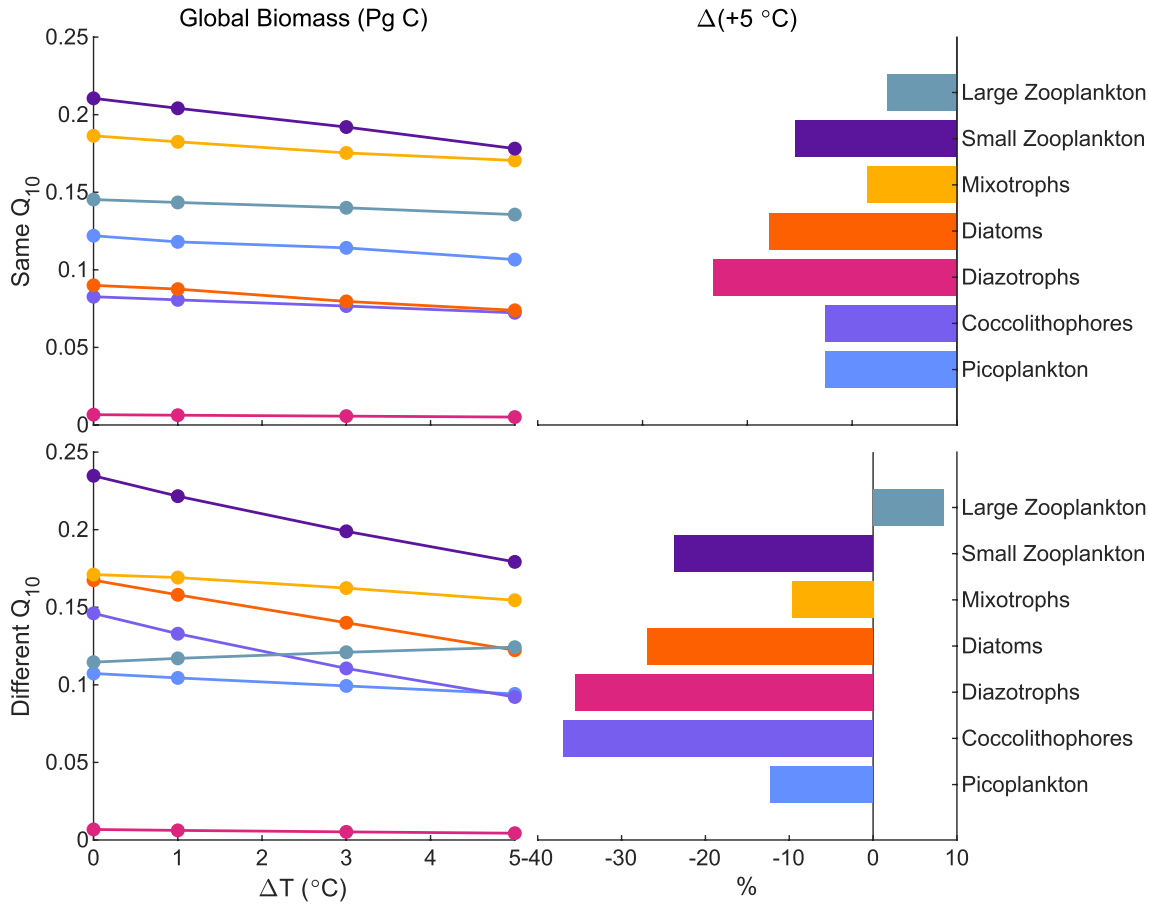

Figure 9. Thermal response for each plankton functional type in the Darwin model. The left column shows the globally integrated biomass of each type as a function of the change in temperature and the right column shows the percent change for each type change between the +0°C and +5°C experiments. All functional types decline with temperature when the Q_{10} values are the same, while the large zooplankton increase when the heterotrophic Q_{10} is larger than the autotrophic Q_{10}. In both temperature sensitivity cases, functional types toward the bottom of the food chain tend to decline more than types toward the top, resulting in a proportionally larger fraction of heterotrophs as temperature increases.

The increase in heterotroph to autotroph ratio has biogeochemical consequences as well. Increased zooplankton grazing can have effects on the bottom of the food chain through trophic cascades, and has been shown to reduce both the abundance and diversity of bacterioplankton and inhibit microbially mediated ecosystem services (Zöllner et al., 2009). The shift toward respiration also reduces the efficiency of the biological pump (Barton et al., 2020), which may have compounding effects with other temperature-driven changes, such as the accumulation of dissolved organic carbon compared to particulate (POC; Wohlers-Zöllner et al., 2012). The net result is a shift in marine ecosystems toward bacteria-dominated systems that recycle carbon in the surface ocean rather than export carbon via the biological pump. A reduction in the carbon export flux has been described more broadly as a consequence of warming (Long et al., 2021; Wohlers et al., 2009). The transient nature of the increased export flux described in this study could represent a temporary re-equilibration event on the way toward steady-state conditions characterized by reduced export.

Transient dynamics were an important component of the results in this study. The decline in total biomass was accounted for with temporary increases in export as a result of the build-up of detritus. The time scale of these transient export events, and the resulting changes in biomass, was on the order of days to weeks. These are significantly smaller time scales than the time scales typically observed in real world trends, which are more likely to be on the order of years to decades (e.g., Behrenfeld et al., 2006). In our models, we employed a very large and instantaneous temperature increase and allowed the ecosystem to re-establish equilibrium. The time scales observed in the model, therefore, represent the biological time scales of the re-equilibration of the ecosystem. In the real world, warming occurs gradually over many years, imposed over a large seasonal signal.

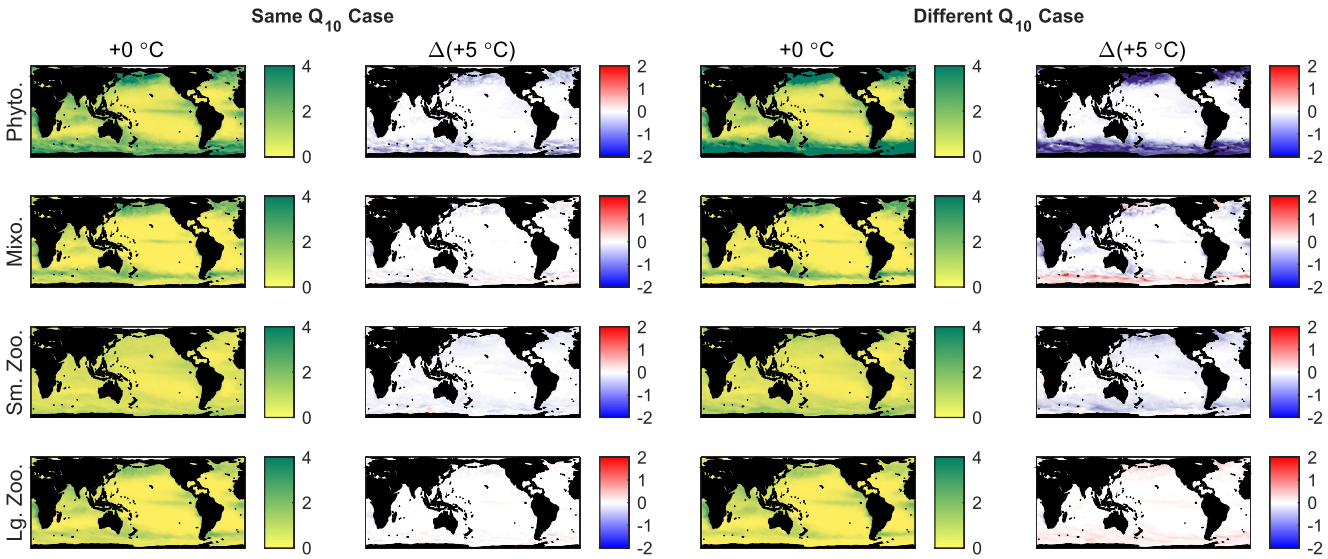

Figure 10. Annual mean depth-integrated biomass (mmol C m^{-2}) in the Darwin model for autotrophic phytoplankton (first row), mixotrophs (second row), and small (third row) and large (fourth row) zooplankton under the two temperature sensitivity scenarios (first column, same Q_{10} values; third column, different Q_{10} values). The net change between the +0°C and +5°C experiments are plotted to quantify the thermal response of each variable. The Data are from the tenth year of the Darwin model simulations.

Our results suggest that the time scale of the ecosystem response is quite small relative to the time scale of the driver, so empirically observed ecosystem trends likely represent quasi-steady states and not transient responses to perturbation.

The magnitude of the ecosystem thermal response depends, in large part, upon the assumption made concerning the temperature sensitivity of various metabolic processes. In both the Darwin and the box model simulations, ecosystems had greater sensitivity to temperature if the Q_{10} values differed across different metabolic processes. Here, we compared the case in which all the Q_{10} values in the model are equal against the case in which the Q_{10} for heterotrophic metabolic processes is higher than that of autotrophic processes. These assumptions were based on empirical evidence that show increased temperature sensitivity in the growth rates of heterotrophs (Rose & Caron, 2007). However, our knowledge of the variability in real world Q_{10} is incomplete. Temperature sensitivity certainly varies across phytoplankton taxa (Anderson et al., 2021) and between phytoplankton and zooplankton (Eppley, 1972; Rose & Caron, 2007), but the variability in temperature sensitivity for other important ecosystem rates, including mortality and remineralization, and the regional variability across biogeochemical regimes remains largely undescribed. Our results suggest that this variability in temperature sensitivity may have significant effects on the thermal sensitivity of the ecosystem as a whole. A more complete understanding of how specific biological rates depend on temperature will provide insight into the sensitivity of ocean biogeochemical fluxes (Riebesell et al., 2009). A better description of the variance in Q_{10} coefficients between different taxa and biogeochemical regimes will expand our understanding of how marine ecosystems will respond to warming and should be a priority in future research (Edwards et al., 2016; Sherman et al., 2016).

It is important to note that these temperature sensitivities are likely not fixed (Marañón et al., 2018). Organisms adapt to their environment and evolution in response to warming may function to modulate the ecosystem response (Padfield et al., 2016). Increased thermal diversity has been shown to dampen ecosystem thermal sensitivity because communities are better able to track temperature fluctuations in the environment (Chen, 2022). A "flattening" of the Q_{10} curves via adaptation could reduce the temperature sensitivity of ecosystems and lead to smaller thermal responses (Bishop et al., 2022; Ward et al., 2019). Notably, the capacity for some phytoplankton communities to adapt to rising temperatures may be limited in regions with the highest mean temperatures since these species are already living in conditions approaching their thermal maxima (Thomas et al., 2012). This physiological restriction may make tropical species more vulnerable to warming and result in reductions in phytoplankton diversity near the equator (Deutsch et al., 2008; Thomas et al., 2012).

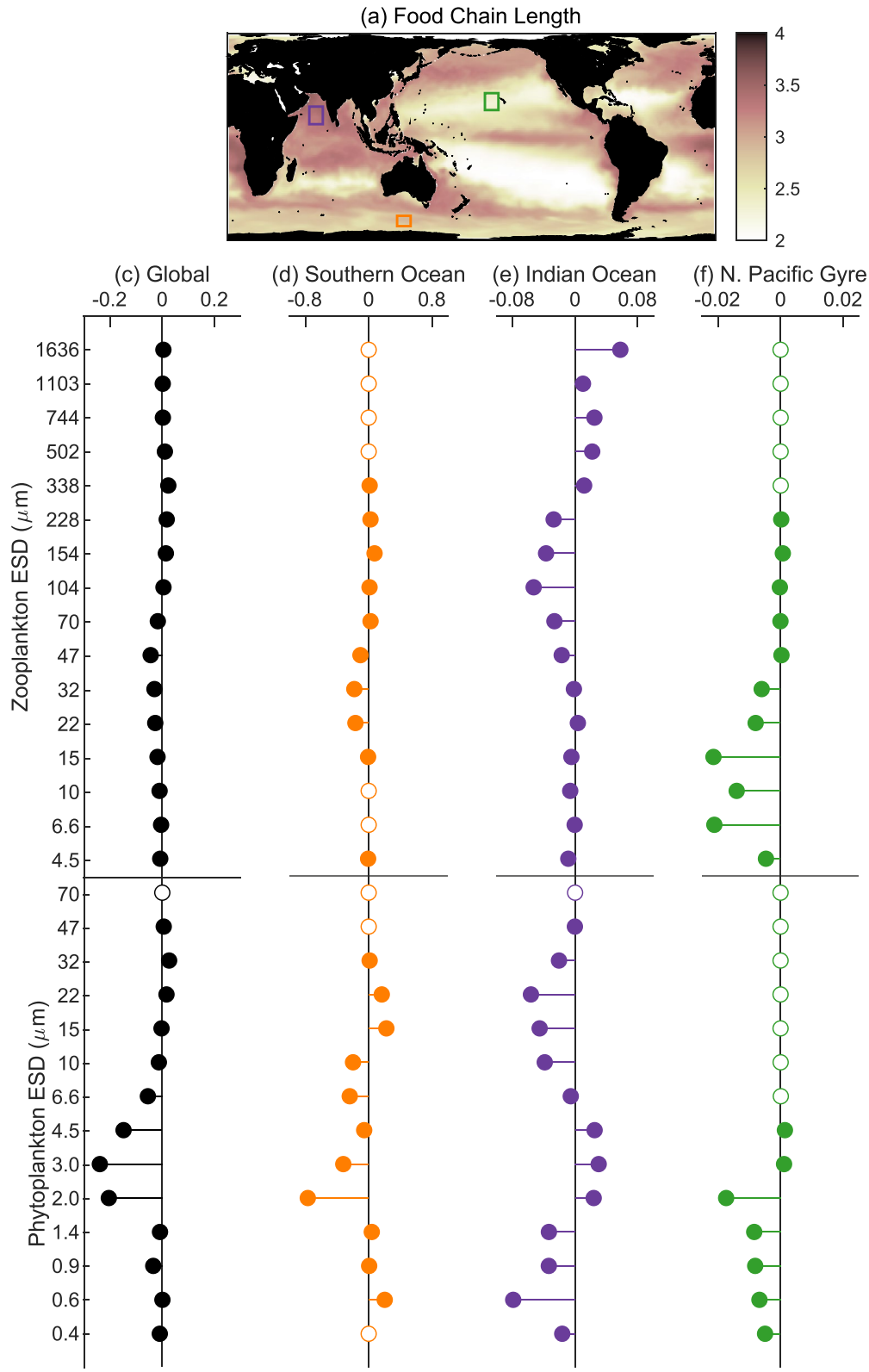

Figure 11. (a) Global variability in food chain length in the tenth year of the Darwin model simulation, under the assumption that the heterotrophic Q_{10} value is higher than the autotrophic value (Exp. 5 in Table 1). Shown in the lower panels are the size class-specific biomass changes (depth-integrated; mmol C m^{-2}) between the +0°C and +5°C experiments for the following regions: (c) the global mean, (d) the Southern Ocean, (e) the Indian Ocean, and (f) the North Pacific gyre. Open circles indicated size classes that fall below a concentration threshold of 10^{-4} mmol C m^{-3}.

This study has particular relevance to ESMs, including those used in the IPCC CMIP ensembles. These models include Q_{10} parameterizations of temperature sensitivity for biological rates, and as such the mechanisms we describe in this study will be at play in their future change scenarios. These mechanisms, including the direct effects of temperature on NPP and biomass and the shift in the heterotroph to autotroph ratio, will occur in their projections, but they have not been isolated before. Other effects such as alterations in nutrient supplies and light environment will occur in the ESM as well. The combination of all these stressors will lead to different outcomes in different regions (see e.g., Dutkiewicz et al., 2013). But no previous study has focused on the plankton community consequences as found in this study.

The Darwin model's sensitivity to assumptions concerning Q_{10} values may therefore also provide insight into the differences in results from various ESMs. There is a high degree of variability among the ESMs participating in CMIP6, with disagreement in the sign of the ecosystem response over the twenty-first century in many locations (Henson et al., 2022; Kwiatkowski et al., 2020). Some of this uncertainty likely arises from differences in the implementation of temperature sensitivity, varying from using the same sensitivity for all plankton types (e.g., GFDL-COBALT; Stock et al., 2020), to using different Q_{10} values for phyto- and zooplankton (e.g., IPSL-PISCES; Aumont et al., 2015), to implementing phytoplankton temperature dependent but zooplankton independent (e.g., UK-ESM-MEDUSA; Yool et al., 2013). The lack of consistency could at least partially be due to the mechanisms described here, which are already at work in the CMIP6 models, albeit alongside other sources of ecosystem change.

We have taken a diagnostic approach in our modeling method and worked to isolate one mechanism of temperature-driven ecosystem change that arises from the direct effects of temperature on metabolism. However, it is important to acknowledge that this mechanism exists in the context of a suite of direct and indirect effects that temperature has on marine food webs. These effects include changes to water column structure and stratification, changes to circulation at multiple scales, and ocean acidification (Behrenfeld et al., 2006; Dutkiewicz et al., 2019, 2015, 2013; Falkowski et al., 1998; Martinez et al., 2009). Multiple, simultaneous mechanisms of ecosystem change will alter nutrient availability, biomass, and community structure in complex ways. Ecosystem-level thermal responses are therefore an emergent behavior of a complex assemblage of temperature-driven changes to both physics and biology in the ocean. A complete understanding of ecosystem thermal sensitivity is an iterative and ongoing process of building up layers of understanding of individual mechanisms of change and how they interact. The purpose of this study was specifically to examine the thermal response of metabolism, an effect that is present in previous models, but not fully examined.

Data Availability Statement

The code and specific parameters and simulation output used in this study are available at Harvard Dataverse under DOI https://doi.org/10.7910/DVN/NEVQZI (Archibald et al., 2022).

Acknowledgments

Work was supported by the US National Science Foundation (OCE-1851194 to HVM) and by the Simons Foundation (Award 689265 to HVM). S.D. is grateful for support from the Simons Collaboration on Computational Biogeochemical Modeling of Marine Ecosystems (CBIOMES; Simons Foundation Grant 549931) and from NASA (Grant 80NSSC22K0153). C.L. acknowledges support from the Swiss National Science Foundation (Grant 174124). We thank Suzana Leles, Ferdinand Pfab, and members of the Moeller lab for comments on earlier versions of this manuscript. Special thanks to Elise Cypher for scientific illustrations.

References

Anderson, S. I., Barton, A. D., Clayton, S., Dutkiewicz, S., & Rynearson, T. A. (2021). Marine phytoplankton functional types exhibit diverse responses to thermal change. *Nature Communications*, *12*, 1–9. https://doi.org/10.1038/s41467-021-26651-8

Archibald, K. M., Dutkiewicz, S., Laufkötter, C., & Moeller, H. V. (2022). Thermal responses in global marine planktonic food webs mediated through temperature effects on metabolism [Dataset]. DARWIN Project Dataverse. Retrieved from https://dataverse.harvard.edu/dataverse/darwin

Aumont, O., Ethé, C., Tagliabue, A., Bopp, L., & Gehlen, M. (2015). PISCES-v2: An ocean biogeochemical model for carbon and ecosystem studies. *Geoscientific Model Development*, *8*, 2465–2513. https://doi.org/10.5194/gmd-8-2465-2015

Barton, S., Jenkins, J., Buckling, A., Schaum, C. E., Smirnoff, N., Raven, J. A., & Yvon-Durocher, G. (2020). Evolutionary temperature compensation of carbon fixation in marine phytoplankton. *Ecology Letters*, *23*(4), 722–733. https://doi.org/10.1111/ele.13469

Barton, S., & Yvon-Durocher, G. (2019). Quantifying the temperature dependence of growth rate in marine phytoplankton within and across species. *Limnology & Oceanography*, *64*(5), 2081–2091. https://doi.org/10.1002/lno.11170

Behrenfeld, M. J., O'Malley, R. T., Siegel, D. A., McClain, C. R., Sarmiento, J. L., Feldman, G. C., et al., (2006). Climate-driven trends in contemporary ocean productivity. *Nature*, *444*(7120), 752–755. https://doi.org/10.1038/nature05317

Benedetti, F., Vogt, M., Elizondo, U. H., Righetti, D., Zimmermann, N. E., & Gruber, N. (2021). Major restructuring of marine plankton assemblages under global warming. *Nature Communications*, *12*, 1–15. https://doi.org/10.1038/s41467-021-25385-x

Bindoff, N. L., Artale, V., Cazenave, A., Gregory, J. M., Willebrand, J., Artale, V., et al. (2007). Observations: Oceanic climate change and sea level. In S. Solomon et al. (Eds.) *Climate change 2007: The physical science basis*. Cambridge University Press.

Bishop, I. W., Anderson, S. I., Collins, S., & Rynearson, T. A. (2022). Thermal trait variation may buffer Southern Ocean phytoplankton from anthropogenic warming. *Global Change Biology*, *28*(19), 5755–5767. https://doi.org/10.1111/gcb.16329

Bissinger, J. E., Montagnes, D. J. S., Sharples, J., & Atkinson, D. (2008). Predicting marine phytoplankton maximum growth rates from temperature: Improving on the Eppley curve using quantile regression. *Limnology & Oceanography*, *53*(2), 487–493. https://doi.org/10.4319/lo.2008.53.2.0487

Bopp, L., Aumont, O., Cadule, P., Alvain, S., & Gehlen, M. (2005). Response of diatoms distribution to global warming and potential implications: A global model study. *Geophysical Research Letters*, *32*(19), 1–4. https://doi.org/10.1029/2005GL023653

Bopp, L., Resplandy, L., Orr, J. C., Doney, S. C., Dunne, J. P., Gehlen, M., et al. (2013). Multiple stressors of ocean ecosystems in the 21st century: Projections with CMIP5 models. *Biogeosciences*, *10*, 6225–6245. https://doi.org/10.5194/bg-10-6225-2013

Boyce, D. G., Lewis, M. R., & Worm, B. (2010). Global phytoplankton decline over the past century. *Nature*, *466*(7306), 591–596. https://doi.org/10.1038/nature09268

Buitenhuis, E. T., Vogt, M., Moriarty, R., Bednaršek, N., Doney, S. C., Leblanc, K., et al. (2013). MAREDAT: Toward a world atlas of MARine ecosystem DATa. *Earth System Science Data*, *5*(2), 227–239. https://doi.org/10.5194/essd-5-227-2013

Chen, B. (2022). Thermal diversity affects community responses to warming. *Ecological Modeling*, *464*, 109846. https://doi.org/10.1016/j.ecolmodel.2021.109846

Cheng, L., Abraham, J., Hausfather, Z., & Trenberth, K. E. (2019). How fast are the oceans warming? *Science*, *363*(6423), 128–129. https://doi.org/10.1126/science.aav7619

Deutsch, C. A., Tewksbury, J. J., Huey, R. B., Sheldon, K. S., Ghalambor, C. K., Haak, D. C., & Martin, P. R. (2008). Impacts of climate warming on terrestrial ectotherms across latitude. *Proceedings of the National Academy of Sciences*, *105*(18), 6668–6672. https://doi.org/10.1073/pnas.0709472105

Dutkiewicz, S., Cermeno, P., Jahn, O., Follows, M. J., Hickman, A. A., Taniguchi, D. A., & Ward, B. A. (2020). Dimensions of marine phytoplankton diversity. *Biogeosciences*, *17*(3), 609–634. https://doi.org/10.5194/bg-17-609-2020

Dutkiewicz, S., Hickman, A. E., Jahn, O., Henson, S., Beaulieu, C., & Monier, E. (2019). Ocean color signature of climate change. *Nature Communications*, *10*, 1–13. https://doi.org/10.1038/s41467-019-08457-x

Dutkiewicz, S., Morris, J. J., Follows, M. J., Scott, J., Levitan, O., Dyhrman, S. T., & Berman-Frank, I. (2015). Impact of ocean acidification on the structure of future phytoplankton communities. *Nature Climate Change*, *5*(11), 1002–1006. https://doi.org/10.1038/nclimate2722

Dutkiewicz, S., Scott, J. R., & Follows, M. J. (2013). Winners and losers: Ecological and biogeochemical changes in a warming ocean. *Global Biogeochemical Cycles*, *27*(2), 463–477. https://doi.org/10.1002/gbc.20042

Edwards, K. F., Thomas, M. K., Klausmeier, C. A., & Litchman, E. (2016). Phytoplankton growth and the interaction of light and temperature: A synthesis at the species and community level. *Limnology & Oceanography*, *61*(4), 1232–1244. https://doi.org/10.1002/lno.10282

Eppley, R. W. (1972). Temperature and phytoplankton growth in the sea. *Fishery Bulletin*, *70*, 1063–1085.

Falkowski, P. G., Barber, R. T., & Smetacek, V. (1998). Biogeochemical controls and feedbacks on ocean primary production. *Science*, *281*(5374), 200–2006. https://doi.org/10.1126/science.281.5374.200

Follett, C. L., Dutkiewicz, S., Ribalet, F., Zakem, E., Caron, D., Armbrust, E. V., & Follows, M. J. (2022). Trophic interactions with heterotrophic bacteria limit the range of *Prochlorococcus*. *Proceedings of the National Academy of Sciences*, *119*(2). https://doi.org/10.1073/pnas.2110993118/-/DCSupplemental

Frölicher, T. L., Fischer, E. M., & Gruber, N. (2018). Marine heatwaves under global warming. *Nature*, *560*(7718), 360–364. https://doi.org/10.1038/s41586-018-0383-9

Gardner, J. L., Peters, A., Kearney, M. R., Joseph, L., & Heinsohn, R. (2011). Declining body size: A third universal response to warming? *Trends in Ecology & Evolution*, *26*(6), 285–291. https://doi.org/10.1016/j.tree.2011.03.005

Geider, R. J., Maclntyre, H. L., & Kana, T. M. (1998). A dynamic regulatory model of phytoplanktonic acclimation to light, nutrients, and temperature. *Limnology & Oceanography*, *43*(4), 679–694. https://doi.org/10.4319/lo.1998.43.4.0679

Gilbert, B., Tunney, T. D., Mccann, K. S., Delong, J. P., Vasseur, D. A., Savage, V., et al. (2014). A bioenergetic framework for the temperature dependence of trophic interactions. *Ecology Letters*, *17*(8), 902–914. https://doi.org/10.1111/ele.12307

Hansen, P. J., Bjørnsen, P. K., & Hansen, B. W. (1997). Zooplankton grazing and growth: Scaling within the 2–2,000 μm body size range. *Limnology & Oceanography*, *42*(4), 687–704. https://doi.org/10.4319/lo.1997.42.4.0687

Henson, S. A., Laufkötter, C., Leung, S., Giering, S. L., Palevsky, H. I., & Cavan, E. L. (2022). Uncertain response of ocean biological carbon export in a changing world. *Nature Geoscience*, *15*(4), 248–254. https://doi.org/10.1038/s41561-022-00927-0

Henson, S. A., Sarmiento, J. L., Dunne, J. P., Bopp, L., Lima, I., Doney, S. C., et al. (2010). Detection of anthropogenic climate change in satellite records of ocean chlorophyll and productivity. *Biogeosciences*, *7*(2), 621–640. https://doi.org/10.5194/bg-7-621-2010

Holling, C. S. (1965). The functional response of predators to prey density and its role in mimicry and population regulation. *Memoirs of the Entomological Society of Canada*, *97*(S45), 5–60. https://doi.org/10.4039/entm9745fv

Huntley, M. E., & Lopez, M. D. (1992). Temperature-dependent production of marine copepods: A global synthesis. *The American Naturalist*, *140*(2), 201–242. https://doi.org/10.1086/285410

Irwin, A. J., & Oliver, M. J. (2009). Are ocean deserts getting larger? *Geophysical Research Letters*, *36*(18), L18609., https://doi.org/10.1029/2009GL039883

Kiørboe, T. (2018). *A mechanistic approach to plankton ecology*. Princeton University Press.

Klauschies, T., Bauer, B., Aberle-Malzahn, N., Sommer, U., & Gaedke, U. (2012). Climate change effects on phytoplankton depend on cell size and food web structure. *Marine Biology*, *159*(11), 2455–2478. https://doi.org/10.1007/s00227-012-1904-y

Kwiatkowski, L., Torres, O., Bopp, L., Aumont, O., Chamberlain, M., Christian, J. R., et al. (2020). Twenty-first century ocean warming, acidification, deoxygenation, and upper-ocean nutrient and primary production decline from CMIP6 model projections. *Biogeosciences*, *17*(13), 3439–3470. https://doi.org/10.5194/bg-17-3439-2020

Laufkötter, C., Vogt, M., Gruber, N., Aita-Noguchi, M., Aumont, O., Bopp, L., et al. (2015). Drivers and uncertainties of future global marine primary production in marine ecosystem models. *Biogeosciences*, *12*(23), 6955–6984. https://doi.org/10.5194/bg-12-6955-2015

Laufkötter, C., Zscheischler, J., & Frölicher, T. L. (2020). High-impact marine heatwaves attributable to human-induced global warming. *Science*, *369*(6511), 1621–1625. https://doi.org/10.1126/science.aba0690

Lewandowska, A. M., & Sommer, U. (2010). Climate change and the spring bloom: A mesocosm study on the influence of light and temperature on phytoplankton and mesozooplankton. *Marine Ecology Progress Series*, *405*, 101–111. https://doi.org/10.3354/meps08520

Lewandowska, A. M., Boyce, D. G., Hofmann, M., Matthiessen, B., Sommer, U., & Worm, B. (2014). Effects of sea surface warming on marine plankton. *Ecology Letters*, *17*(5), 614–623. https://doi.org/10.1111/ele.12265

Long, M. C., Moore, J. K., Lindsay, K., Levy, M., Doney, S. C., Luo, J. Y., et al. (2021). Simulations with the Marine Biogeochemistry Library (MARBL). *Journal of Advances in Modeling Earth Systems*, *13*(12). https://doi.org/10.1029/2021MS002647

López-Urrutia, A. A., Martin, E. S., Harris, R. P., & Irigoien, X. (2006). Scaling the metabolic balance of the oceans. *Proceedings of the National Academy of Sciences*, *103*(23), 8739–8744. https://doi.org/10.1073/pnas.0601137103

Marañón, E., Lorenzo, M. P., Cermeño, P., & Mouriño-Carballido, B. (2018). Nutrient limitation suppresses the temperature dependence of phytoplankton metabolic rates. *The ISME Journal*, *12*(7), 1836–1845. https://doi.org/10.1038/s41396-018-0105-1

Marshall, J., Adcroft, A., Hill, C., Perelman, L., & Heisey, C. (1997). A finite-volume, incompressible Navier Stokes model for, studies of the ocean on parallel computers. *Journal of Geophysical Research C: Oceans*, *102*(C3), 5753–5766. https://doi.org/10.1029/96JC02775

Martinez, E., Antoine, D., & Gentili, B. (2009). Climate-driven basin-scale decadal oscillations of oceanic phytoplankton. *Science*, *326*(5957), 1253–1256. https://doi.org/10.1126/science.1177012

Morán, X. A. G., López-Urrutia, Á., Calvo-Díaz, A., & Li, W. K. (2010). Increasing importance of small phytoplankton in a warmer ocean. *Global Change Biology*, *16*(3), 1137–1144. https://doi.org/10.1111/j.1365-2486.2009.01960.x

Murphy, G. E., Romanuk, T. N., & Worm, B. (2020). Cascading effects of climate change on plankton community structure. *Ecology and Evolution*, *10*(4), 2170–2181. https://doi.org/10.1002/ece3.6055

O'Connor, M. I. (2009). Warming strengthens an herbivore-plant interaction. *Ecology*, *90*(2), 388–398. https://doi.org/10.1890/08-0034.1

O'Connor, M. I., Piehler, M. F., Leech, D. M., Anton, A., & Bruno, J. F. (2009). Warming and resource availability shift food web structure and metabolism. *PLoS Biology*, *7*(8), e1000178. https://doi.org/10.1371/journal.pbio.1000178

Padfield, D., Yvon-Durocher, G., Buckling, A., Jennings, S., & Yvon-Durocher, G. (2016). Rapid evolution of metabolic traits explains thermal adaptation in phytoplankton. *Ecology Letters*, *19*(2), 133–142. https://doi.org/10.1111/ele.12545

Polovina, J. J., Howell, E. A., & Abecassis, M. (2008). Ocean's least productive waters are expanding. *Geophysical Research Letters*, *35*(3), L03618. https://doi.org/10.1029/2007GL031745

Riebesell, U., Körtzinger, A., & Oschlies, A. (2009). Sensitivities of marine carbon fluxes to ocean change. *Proceedings of the National Academy of Sciences*, *106*(49), 20602–20609. https://doi.org/10.1073/pnas.0813291106

Rose, J. M., & Caron, D. A. (2007). Does low temperature constrain the growth rates of heterotrophic protists? Evidence and implications for algal blooms in cold waters. *Limnology & Oceanography*, *52*(2), 886–895. https://doi.org/10.4319/lo.2007.52.2.0886

Schartau, M., Landry, M. R., & Armstrong, R. A. (2010). Density estimation of plankton size spectra: A reanalysis of IronEx II data. *Journal of Plankton Research*, *32*(8), 1167–1184. https://doi.org/10.1093/plankt/fbq072

Sherman, E., Moore, J. K., Primeau, F., & Tanouye, D. (2016). Temperature influence on phytoplankton community growth rates. *Global Biogeochemical Cycles*, *30*(4), 550–559. https://doi.org/10.1002/2015GB005272

Stock, C. A., Dunne, J. P., Fan, S., Ginoux, P., John, J., Krasting, J. P., et al. (2020). Ocean biogeochemistry in GFDL's Earth System Model 4.1 and its response to increasing atmospheric CO_2. *Journal of Advances in Modeling Earth Systems*, *12*(10). https://doi.org/10.1029/2019MS002043

Taucher, J., & Oschlies, A. (2011). Can we predict the direction of marine primary production change under global warming? *Geophysical Research Letters*, *38*(2). https://doi.org/10.1029/2010GL045934

Thomas, M. K., Kremer, C. T., Klausmeier, C. A., & Litchman, E. (2012). A global pattern of thermal adaptation in marine phytoplankton. *Science*, *338*(6110), 1085–1088. https://doi.org/10.1126/science.1224836

Ward, B. A. (2015). Temperature-correlated changes in phytoplankton community structure are restricted to polar waters. *PLoS One*, *10*(8), e0135581. https://doi.org/10.1371/journal.pone.0135581

Ward, B. A., Collins, S., Dutkiewicz, S., Gibbs, S., Bown, P., Ridgwell, A., et al. (2019). Considering the role of adaptive evolution in models of the ocean and climate system. *Journal of Advances in Modeling Earth Systems*, *11*, 3343–3361. https://doi.org/10.1029/2018MS001452

Westerling, A. L., Hidalgo, H. G., Cayan, D. R., & Swetnam, T. W. (2006). Warming and earlier spring increase western U.S. forest wildfire activity. *Science*, *313*(5789), 940–943. https://doi.org/10.1126/science.1128834

Winder, M., & Sommer, U. (2012). Phytoplankton response to a changing climate. *Hydrobiologia*, *698*(1), 5–16. https://doi.org/10.1007/s10750-012-1149-2

Wohlers, J., Engel, A., Breithaupt, P., Jürgens, K., Hoppe, H.-G., Sommer, U., & Riebesell, U. (2009). Changes in biogenic carbon flow in response to sea surface warming. *Proceedings of the National Academy of Sciences*, *106*(17), 7067–7072. https://doi.org/10.1073/pnas.0812743106

Wohlers-Zöllner, J., Biermann, A., Engel, A., Dörge, P., Lewandowska, A. M., von Scheibner, M., & Riebesell, U. (2012). Effects of rising temperature on pelagic biogeochemistry in mesocosm systems: A comparative analysis of the AQUASHIFT Kiel experiments. *Marine Biology*, *159*(11), 2503–2518. https://doi.org/10.1007/s00227-012-1958-x

Wunsch, C., & Heimbach, P. (2007). Practical global oceanic state estimation. *Physica D: Nonlinear Phenomena*, *230*(1–2), 197–208. https://doi.org/10.1016/j.physd.2006.09.040

Yool, A., Popova, E. E., & Anderson, T. R. (2013). MEDUSA-2.0: An intermediate complexity biogeochemical model of the marine carbon cycle for climate change and ocean acidification studies. *Geoscientific Model Development*, *6*(5), 1767–1811. https://doi.org/10.5194/gmd-6-1767-2013

Yvon-Durocher, G., Montoya, J. M., Trimmer, M., & Woodward, G. (2011). Warming alters the size spectrum and shifts the distribution of biomass in freshwater ecosystems. *Global Change Biology*, *17*(4), 1681–1694. https://doi.org/10.1111/j.1365-2486.2010.02321.x

Zöllner, E., Hoppe, H.-G., Sommer, U., & Jürgens, K. (2009). Effect of zooplankton-mediated trophic cascades on marine microbial food web components (bacteria, nanoflagellates, ciliates). *Limnology & Oceanography*, *54*(1), 262–275. https://doi.org/10.4319/lo.2009.54.1.0262

Erratum

In the originally published version of this article, Figure 1b was not the final version. Figure 1b has been replaced, and this may be considered the authoritative version of record.